Check for updates

Received: 23 March 2023 | Revised: 30 August 2023

DOI: 10.1002/prep.202300079

Propellants, Explosives, Pyrotechnics

RESEARCH ARTICLE

Enhancement of laser ignitibility of insensitive energetic materials (FOX-7)

Xiao Fang | **Christopher Stennett** | **Sally Gaulter**

Centre for Defence Chemistry, Cranfield University, Defence Academy of the United Kingdom, Shrivenham, UK

Correspondence
Xiao Fang, Centre for Defence Chemistry, Cranfield University, Defence Academy of the United Kingdom, Shrivenham, SN6 8LA, UK.
Email: x.fang@cranfield.ac.uk

Funding information
Dstl UK

Abstract

Experimental investigation into the feasibility of optically sensitising an insensitive explosive, FOX-7 (1,1-Diamino-2,2-dinitroethene) by the doping of gold nanoparticles (GNPs) has been conducted. The commercially available GNPs were specifically designed in their particle shape and size to strongly absorb at the wavelength of the igniting laser (808 nm). The laser ignitibility of FOX-7 was significantly increased as the GNPs efficiently converted the absorbed energy into the heat. The laser ignitibility of such optically sensitised FOX-7 and the detonation capability of the laser initiator devices designed for the study were evaluated. Based on the evaluation of the initiator's output in term of impact pressure, it was shown that an GNPs doped FOX-7 based laser slapper initiator was able to detonate a secondary explosive.

KEYWORDS
explosives, laser ignition, metallic nanoparticles, optical sensitising

1 | INTRODUCTION

Currently used electric initiators of explosive devices usually consist of metal-wire (e.g. bridge-wires) buried in sensitive primary explosive and/or pyrotechnics where high-voltage (or current) electric power is applied to ignite the explosives for the initiation to take place. Main disadvantages of such a technique include: corrosion and surface degradation of the metal components inside explosive materials; impossible maintenance of the metal-wires buried in the explosive; metal-wire being subject to external electromagnetic interference (EMI); high sensitivity of primary explosive to external stimuli [1–4]. These disadvantages could be overcome by using laser for initiation without primary explosives and metal components, which is also partially overcome by exploding film initiation (EFI) using low-sensitive secondary explosive [5]. The use of laser also allows optical shutters to be applied, providing extra safety features. To develop a miniature and practicable laser initiator, a small near-infrared (NIR) diode laser would be the most suitable optical power source due to its miniature size, low cost, commercial availability, and ease of integration. This study aimed to investigate the feasibility of developing a laser initiator for the detonation of secondary explosives.

Insensitive explosives lack sufficient optical ignitibility at NIR wavelength bands due to their low optical absorption [6–9]. It is necessary to modify these materials by incorporating optical sensitisers to enhance the laser ignitibility for effective laser initiation [10–13]. The commonly used optical sensitiser, carbon black, has been widely applied in assisting laser ignition of explosives [10, 12]. However, carbon black absorbs at a broad range of spectrum; its mixtures with explosives are also optically sensitised at undesired light wavelengths, lacking wavelength selectivity. This may raise concerns that sensitised explosives are vulnerable to external optical interference or stimuli during their whole life operation (e.g. manufacturing, storage, transportation). Gold nanoparticles (GNPs) used as an optical sensitiser would allow the design of a wavelength selective optical ignitor that would preferentially respond to laser light within a specific wavelength range. This is attributed to the Surface Plasmon Resonance (SPR) of metallic nanoparticles

 © 2023 Wiley-VCH GmbH.

[14, 15]. GNP was used in this study because it exhibits plasmon resonances at a wavelength within the visible and NIR spectral region, while the other economical metals such as aluminium nanoparticles exhibit SPR within UV spectral region [16–19]. Also, aluminium is easily oxidised and forms an aluminium oxide (Al_2O_3) layer. Therefore, the GNPs are expected to absorb at a specific NIR wavelength (e.g. 808 nm in this study) and efficiently convert the absorbed energy into heat when their frequency band of SPR is comparable to that of igniting laser. Meanwhile, whether GNP's size itself is also a factor to enhance the ignitability in addition to its SPR will remain a further topic in our future research. This SPR absorption maximum can be tuned to a desirable laser wavelength by changing both the size and shape of the nanoparticles [20, 21]. Therefore, GNPs can be efficient optical sensitisers that are wavelength selective. In this study the enhancement of laser ignitibility of explosive FOX-7 by the doping of gold nanoparticles (GNPs) has been achieved using a diode laser at 808 nm wavelength. The laser ignitibility to heat and deflagrate such optically sensitised FOX-7 and the detonation capability of the laser initiator have been evaluated.

2 | EXPERIMENTAL

2.1 | Sample materials and preparation

2.1.1 | Explosive

FOX-7 had particle sizes of 20–40 μm as specified by the manufacturer (Eurenco Bofors, Sweden). FOX-7 chemical structure is shown in Figure 1. The choice of the small sizes was made on the assumption that its mixing with GNPs for optical sensitization would have larger interfacing surface area between the FOX-7 particles and GNPs than those having larger sizes. The explosive characteristics of FOX-7 are listed in Table 1.

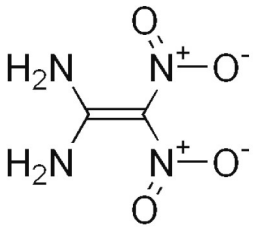

FIGURE 1 Chemical structure of FOX-7.

2.1.1.1 | Optical sensitizers

Rod-shaped gold nanoparticles of 10 nm diameter with 41 nm length have strong optical absorption at 808 nm and were chosen as the sensitizers. The SEM image and absorption spectrum of the GNPs are provided by the manufacturer (Nanopartz, USA) and shown in Figure 2. Two types of samples, Citrate and Cetyltrimethyl ammonium bromide (CTAB) capped GNPs, were procured and received as dispersed in deionised (DI) water. The capping agents (see Figure 3 for the chemical structures) are required to prevent the nanoparticles from aggregation. When mixing with FOX-7, Citrate-capped GNPs may be expected to adsorb on the particle surfaces due to the possible covalently binding of FOX-7 to the GNP's surface, while CTAB-capped GNPs may be freely dispersed on the surfaces of explosive particles.

2.1.1.2 | Sample preparation

Eight different formulations of FOX-7 with GNPs (Citrate capped and CTAB capped and buffered in DI water) were made. The FOX-7 was weighed into an ample vial, and the required quantity of GNP dispersion was dispensed into the glass vial. The slurry was mixed to ensure the explosive particles and the gold particles were dispersed homogeneously. The glass vials were left in the fume cupboard to allow the liquid dispersant (water) to evaporate. The explosive mixes were stirred daily to prevent caking and settlement of the gold before they were dry. Once the samples looked dry (free flowing) they were placed in a vacuum desiccator overnight. The samples of FOX-7 mixtures with GNPs were made ready for testing, as listed in Table 2.

TABLE 1 Characteristics of FOX-7.

Density: 1.885 g cm^{-3}	Sensitivity ESD (Bofors): > 8 J
Heat of formation: 8 kJ mol^{-1}	Auto-ignition temperature: 215 °C
Friction sensitivity (ISF): > 350 N (RDX: 120 N)	Detonation pressure: 34 GPa (RDX: 35 GPa)
Impact sensitivity (ISI): 20–40 J (RDX: 4–5 J)	Detonation velocity: 8800 m s^{-1} (RDX: 8930 m s^{-1})

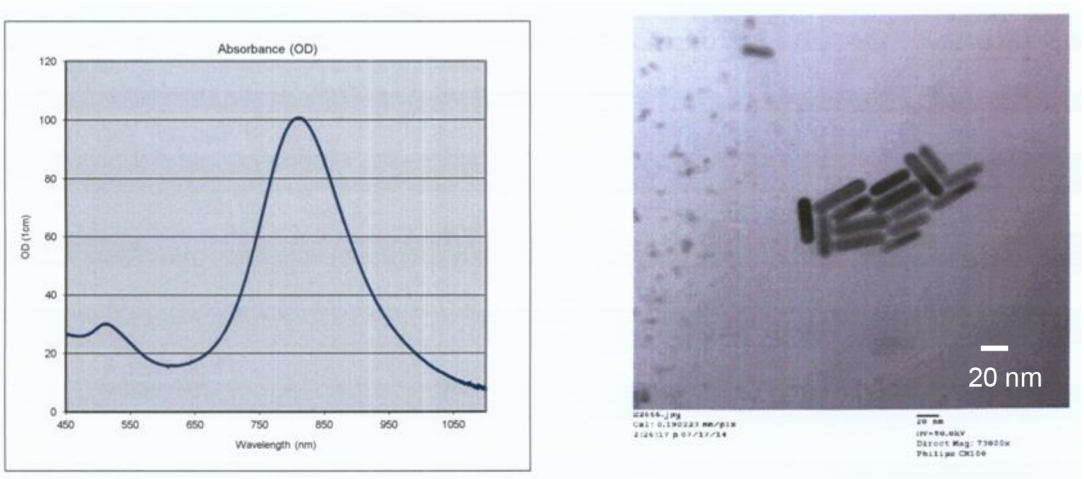

FIGURE 2 Absorption spectrum and SEM image of GNPs used in this study.

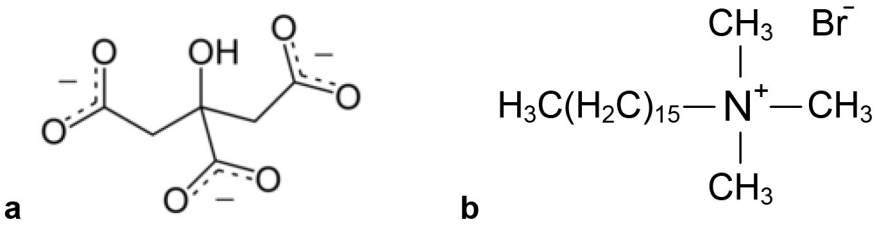

FIGURE 3 Chemical structures of the capping agents: a) Citrate and b) CTAB.

TABLE 2 FOX-7 mixtures with GNPs.

Sensitizer used	CTAB capped GNPs				Citrate capped GNPs			
Sample ID	Sa1	Sa2	Sa3	Sa4	Sb1	Sb2	Sb3	Sb4
Concentration (wt.%)	0.01	0.05	0.5	2.0	0.01	0.05	0.5	2.0

2.2 | Experimental set-up

2.2.1 | Optical absorption measurement

The set-up used to measure the optical absorption of the samples at the laser wavelength, 808 nm is shown in Figure 4. The samples (15 mg) were gently pressed, using a clean glass rod, in a small sample glass holder of diameter ~5 mm and depth ~1 mm to create a relatively compact and smooth surface. The filled holder was placed on the sample stage for measurements of their absorption, A, of the incident laser, I_o. The laser beam (0.1 W) was delivered through an optical fiber from the CW diode laser (Jenoptik: JOLD-x-CPXF, Germany) and focused by a 50 mm focal length lens onto the sample surface. The diffuse reflection, I_r and transmission, I_t, of the laser were detected by two photodiodes and the absorption was estimated based on the detected signals and the system calibration procedure. For the measurement, a white powder of $BaSO_4$, a non-absorption material ($A = 0$), was used for the calibration of the incident laser signal, I_o which was the sum of I_r and I_t measured from the $BaSO_4$ powder. The laser absorption, A, is approximately measured by equation (1) below.

$$A = 100\% - I_r/I_o - I_t/I_o. \quad (1)$$

This approximate measurement should be applicable when the angular distributions of diffuse reflection and transmission are respectively assumed the same between those for the calibrating $BaSO_4$ and FOX-7 samples.

2.2.2 | Laser ignition

The experimental set up for the ignition tests for unconfined samples is shown in Figure 5. The diode laser (JOLD-x-CPXF, JENOPTIK, Germany) used in this study

provided power of up to 46 W at 808 nm wavelength. The output of laser power through a 0.4 mm optic fibre core was controlled with the calibrated laser controller (LDC 1000, Laser Electronics). The laser output was in the continuous-wave (CW) mode. The laser beam of Gaussian distribution was focused onto the sample surface to ignite the sample using a lens of 50 mm diameter and 50 mm focal length, and the distance between the lens and the fibre-pigtail end was 70 mm. Based on the geometrical optics, this optical arrangement produces a focal spot of 1 mm in diameter on the focal plane being 175 mm away from the lens. The sample holder was placed on a translator so that the sample surface could be moved up away from the focal plane of the laser beam to increase its spot size on the sample. A typical diameter of 1.5 mm of the beam spot on the sample was checked by firing the laser for 0.1 s at 5 W onto laser absorbing paper and measuring the size of the marked spot with a Vernier microscope. Approximately 6 mg of each sample was filled in one of six holes (3 mm diameter and 2.5 mm deep) in an aluminium block as a sample holder and slightly pressed down for 1.5 mm, using a Perspex hand press, to form a consistent sample volume of 3 mm (diameter)×1 mm (thickness). The light signal of the flame during the ignition process was detected using a photodiode detector (OSRAM Silicon PIN Photodiode: BPX 65) with a rise time of 12 ns. A notch filter (NF808–34, Thorlabs) blocking 808 nm laser radiation was placed in front of this detector to block out any contribution from laser radiation. A digitizing oscilloscope (Hewlett Packard: 5411D) with 600 MHz bandwidth was used to record the temporal history of the ignition process.

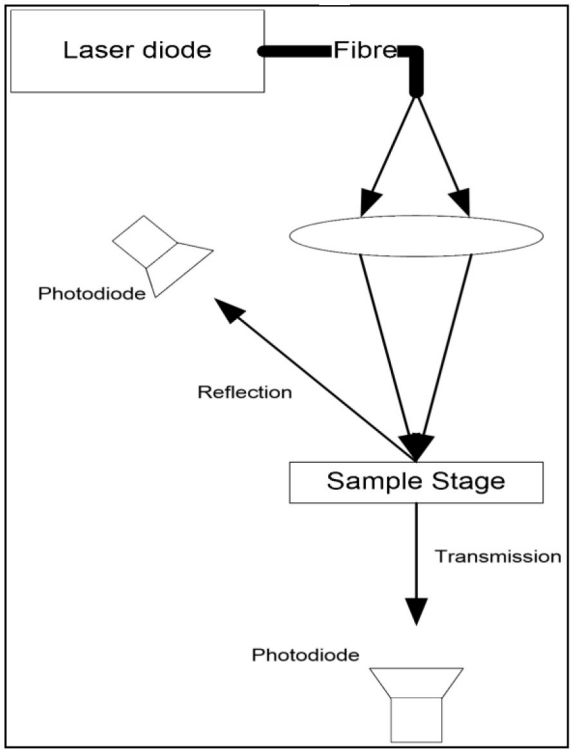

FIGURE 4 Experimental set up for optical absorption measurement.

Laser ignition tests were undertaken over a range of laser powers on the sensitised FOX-7 samples to determine laser ignition threshold, i.e. the minimum laser

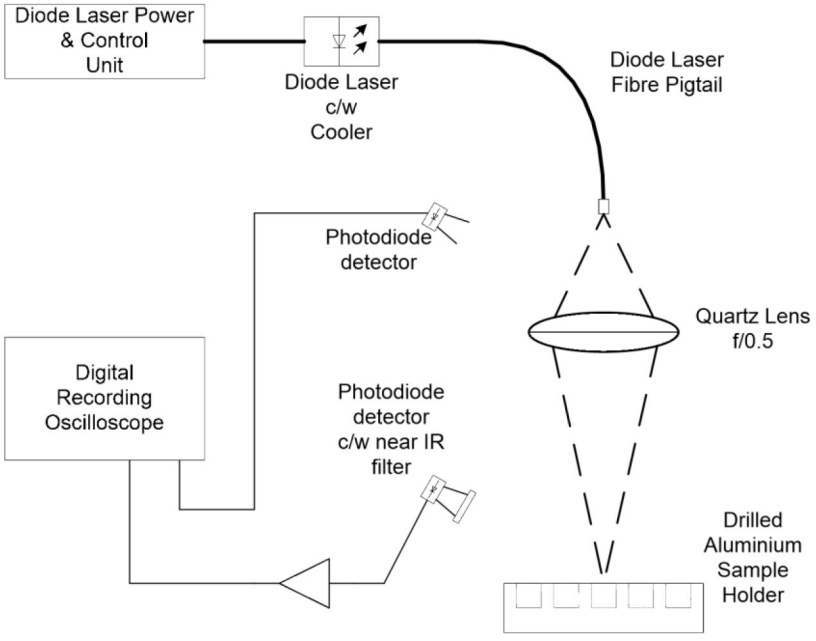

FIGURE 5 Experimental schematics for laser ignition of explosives.

powers required to achieve successful ignition in seven repeated tests using newly loaded samples for each test. After the threshold had been determined, experimentation was conducted above the threshold. Following an ignition, the oscilloscope traces of the ignition signal and igniting laser were recorded. An example is shown in Figure 6, where the measures of ignition delay and full burn delay are defined. The ignition delay is the time duration between the leading edge of the laser pulse and the onset of the ignition process, and the full burn delay is the time duration from the start of ignition to a full burn defined as 90 % of the signal maximum.

2.2.3 | Laser initiator test rig

A test rig was designed to allow firings to be made with the aim to launch a flyer disk at a velocity sufficient to cause initiation in a secondary explosive main charge. Its schematic is shown in Figure 7 and the diagrams showing the general arrangement are given in Figure 8 a and b. The rig consisted of a heavy base plate (1) containing six threaded ports into which the prototype initiators were assembled. A bursting brass disk of 0.2 mm thickness (3) was held in position by a threaded burst disk retainer (2) and provided a cylindrical cavity 5.0 mm in diameter and 4 mm long, into which the explosive components of the prototype could be filled. The upper surface of the explosive cavity was closed by a glass window (4), and this was held in position by a closure plug (5). The closure plug included a hole drilled through its centre, into which the laser fibre could be placed, and ensured that the fibre was centred on the explosive test specimen (6).

The test rig was filled with the explosive components and placed into a clamping jig and the velocity-measuring instrumentation was set up. A photograph of the firing arrangement is shown in Figure 9. The experiments were instrumented with two photodetector cells, positioned so that the time duration between the onset of the laser firing pulse and the ejection of the bursting disk could be measured, which is defined as the initiation delay. The photodiodes (5) and (4), respectively, detect the signals of the laser reflected back from the window glass within the initiator and the laser passing through the initiator after the bursting disk ruptures. In addition, a

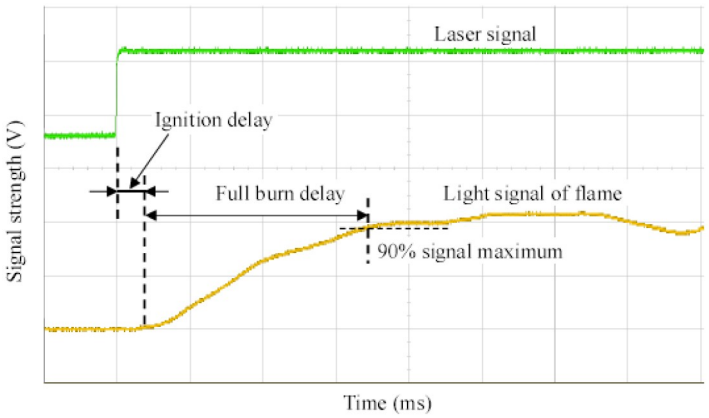

FIGURE 6 Oscilloscope traces of laser and the ignited flame during a laser ignition process, defining the ignition delay and full burn delay.

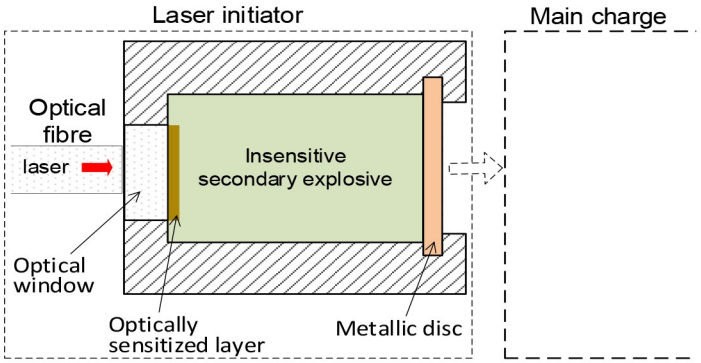

FIGURE 7 A basic schematic of laser initiator (10 mm diameter and 20 mm long).

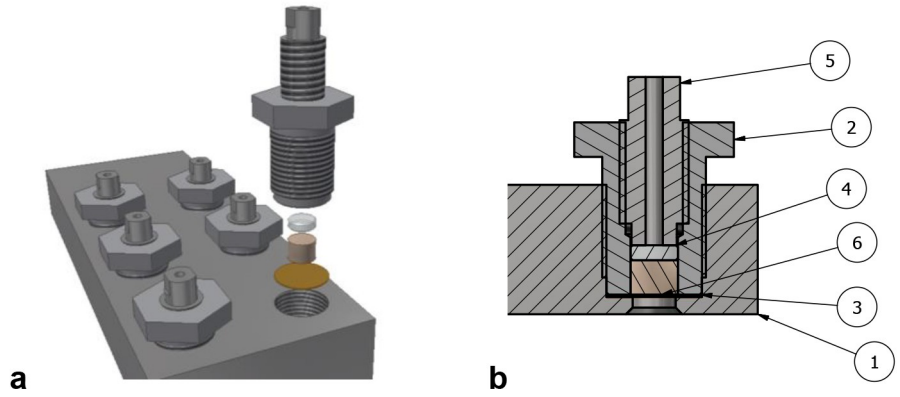

FIGURE 8 a) Exploded diagram overview of initiator test assembly having six test sites, b) Components of the first phase initiator test assembly: 1) base plate, 2) bursting disk retainer, 3) bursting disk, 4) glass window, 5) closure plug, and 6) explosive test specimen.

collimated low-power laser beam was directed at the face of the bursting disk and connected to a laser Doppler interferometer to allow accurate time-resolved measurements of the bursting disk velocity. A short-circuiting pin was used to trigger data capture from the heterodyne velocimeter after the bursting disk had travelled a short (<10 mm) distance. Sufficient firings were successful in obtaining velocity histories.

3. RESULTS AND DISCUSSION

3.1 | Sample analysis

Examples of FOX-7 mixtures with the sensitizers at a concentration of 2 wt.% are shown in Figure 10 along with pure FOX-7. It is noted that the samples became dark coloured which may indicate a better optical absorption. SEM images of FOX-7 mixed with CTAB and Citrate capped GNPs are respectively shown in Figure 11 a and b. As expected, the nanoparticles were adsorbed on the particle surface of the FOX-7 in the mixture of FOX-7/Citrate capped GNPs because of the displacing of Citrate by the amines of FOX-7. In FOX-7/CTAB capped GNPs mixture, nanoparticles were not observed on the particle surface but on the (bottom) sticky surface of sample holder (stub). This was due to the freely dispersed nanoparticles in the mixture being removed by the vacuum pump in the conductivity coating process required for SEM.

3.2 | Optical absorption of the samples

For each sample, the measurement of its optical absorption at 808 nm wavelength was repeated seven times at different spots on the sample surface. The absorption

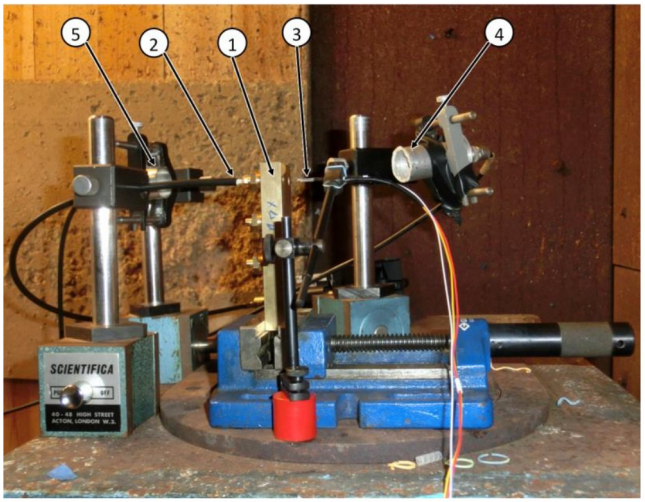

FIGURE 9 Photograph of initiator firing arrangement, showing 1) the initiator assembly; 2) the laser input fibre; 3) the heterodyne velocimeter instrument; (4) and (5) the two photodiodes.

value was an average over these repeated measurements. The results are presented in Table 3. The measurement error is defined as the ratio of the difference between the maximum and the average absorption value to the average value.

The results indicate a large enhancement of optical absorption of the sensitized explosive. At a sensitizer concentration of 2 wt.%, the absorption of sensitized FOX-7 increased from 2.6% for pure FOX-7 to a level of ~60% as highlighted in Table 3. Both Citrate and CTAB capped GNPs generate optical sensitizing effects in the FOX-7. The optical absorption of sensitized FOX-7 with GNPs (citrate and CTAB capped) versus sensitizer concentration (in a log scale) are plotted in Figure 12. It shows that the optical absorption of sensitized FOX-7 increases with the increasing of GNPs' concentration in the explosive.

FIGURE 10 Photos (from left to right) of pure FOX-7 and its mixtures with CTAB and Citrate capped GNPs at 2 wt.% concentration, respectively.

TABLE 3 Optical absorptions for pure and sensitized FOX-7.

Samples	FOX-7	Sa1	Sa2	Sa3	Sa4	Sb1	Sb2	Sb3	Sb4
Optical absorption (%) at 808 nm	**2.6**	7.7	26.4	48.0	**56.7**	16.5	32.9	54.3	**59.9**

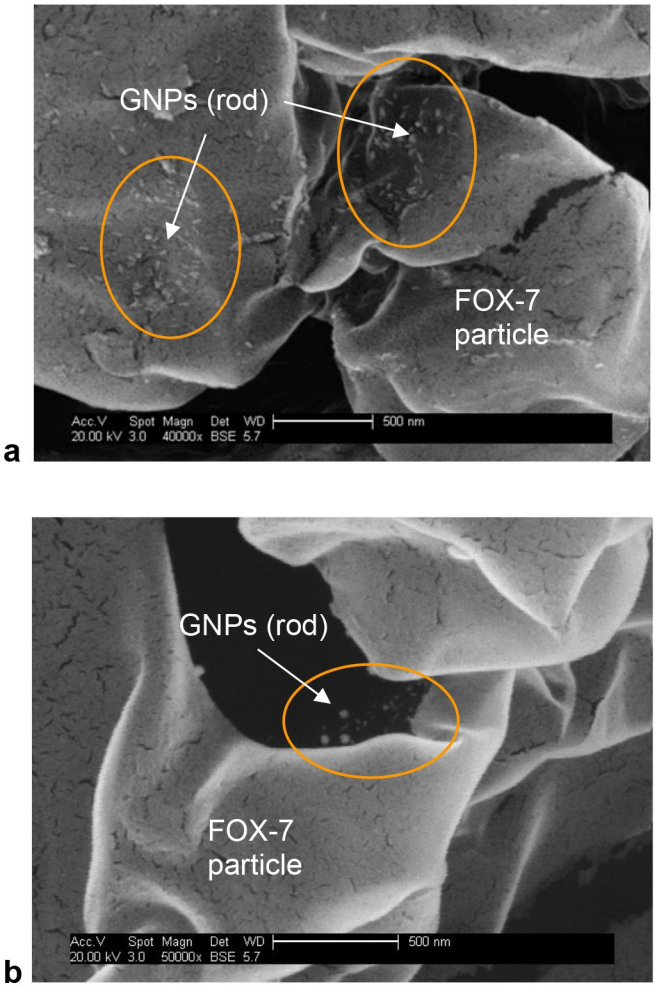

FIGURE 11 SEM images of sensitized FOX-7 with a) Citrate capped GNPs and b) CTAB capped GNPs.

For optical sensitizing of insensitive explosive at 808 nm, the experimental results have proven that GNPs give rise to large enhancement of optical absorption of the explosive when they are specifically designed in their size and shape to have a surface plasmon resonance at the chosen wavelength (as previously shown in Figure 2); the capping agents affect how the GNPs are presented in the sensitized FOX-7, e.g. Citrate capped GNPs adsorb on the particle surfaces of FOX-7 while CTAB capped GNPs freely dispersed in the FOX-7. Optical absorption of the FOX-7 increased to ~60% at a sensitizer concentration of 2 wt.%, and the trends indicate that the absorption increases with higher sensitizer concentrations.

3.3 | Laser ignitability

Optical absorption is a pre-requisite for efficient transfer of laser energy into the bulk of an explosive bed. However, the ignitibility of an explosive will also be governed by thermal properties of the materials and other factors such as sample presentation configurations. The ignition tests were aimed at confirming if GNPs sensitized FOX-7 gives rise to efficient ignition. A series of laser ignition tests were made in an unconfined condition for all samples of sensitized FOX-7. Their laser ignitibility was evaluated in terms of laser ignition threshold, ignition delay and the effects of the laser beam and sample compactness.

The pure FOX-7 without optical sensitization was not ignitable with a laser power output of up to 46 W (the available maximum for this study) with a laser beam spot of ~1.5 mm in diameter and laser duration 100 ms which was used for all the sensitized samples. The laser ignition threshold powers were tested for the sensitized FOX-7, as shown in Table 4. It was found that the

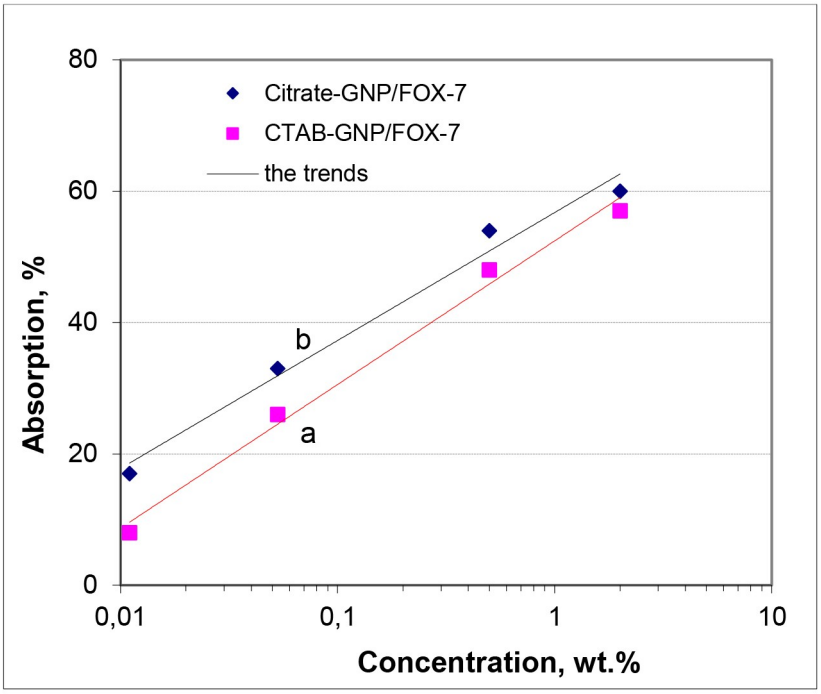

FIGURE 12 Optical absorption of sensitized FOX-7 vs concentration of GNPs capped with a) CTAB and b) Citrate.

TABLE 4 Threshold power of laser ignition.

	Threshold power (W)	
Sensitizer concentration (wt.%)	**CTAB/GNPs**	**Citrate/GNPs**
0 (Pure Fox-7)	Not ignitable (> 46 W)	
0.01	Not ignitable	Not ignitable
0.05	40	Not ignitable
0.5	17	Not ignitable
2	8	25

samples sensitized with Citrate capped GNPs at lower concentrations ≤ 0.5 wt.% (i.e. Sb1, Sb2 and Sb3) and CTAB capped GNPs at 0.01 wt.% (i.e. Sa1) were not ignitable. The results at 2 wt.% sensitizer concentration show that the threshold power (~8 W) to ignite the sensitized FOX-7 with CTAB capped GNPs was much lower than those (25 W and 30 W) for Citrate capped GNPs. A plot of the threshold power against sensitizer concentrations of CTAB capped GNPs is shown in Figure 13. It indicates that the required laser power to ignite the sensitized FOX-7 was largely reduced as the concentration was increased, and the trend predicts a further reduction in the ignition power if a higher concentration of the sensitizer is applied to FOX-7.

To compare the ignition performance for the two sensitizers, when added in 2 wt.%, ignition delay time was measured and plotted against the laser power applied in each ignition process. This plot, as shown in Figure 14, is also known as the 'Ignition map'. The map shows a rapid decrease of ignition delay as the laser power increases for both of the sensitizers. When the laser power increased to 46 W (the available maximum power), the ignition delay time reduced to ~11 ms for CTAB capped GNPs and ~26 ms for Citrate capped GNPs. Based on the results of lower threshold power and shorter ignition delay, CTAB capped GNPs is a better optical sensitizer for FOX-7 and was used for the later tests. The better ignitibility in use of CTAB capped GNPs may be due to the heat transfer between the GNPs and the FOX-7 particles; but the causes for this would be investigated in our future research.

To determine the optimum laser beam size for the ignition, four different beam sizes were used at a laser power of 46 W. The ignition delay time was measured

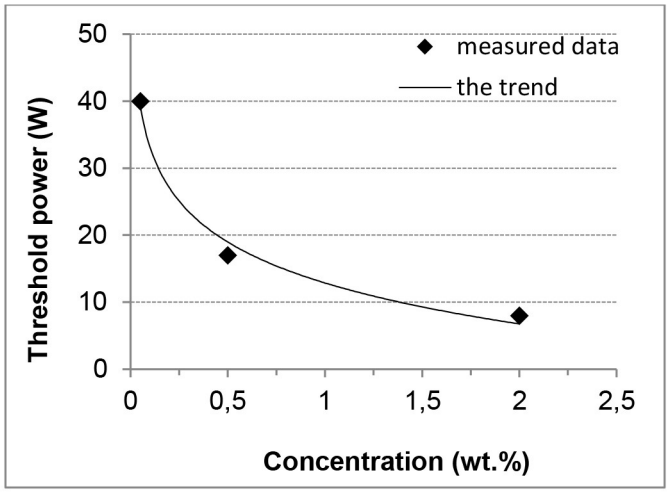

FIGURE 13 Laser ignition threshold power required for varying CTAB/GNP concentrations.

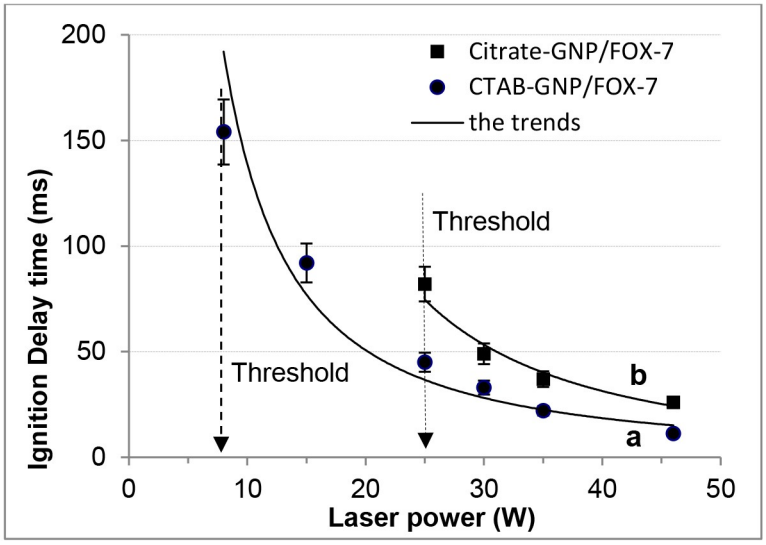

FIGURE 14 Ignition delay time vs laser power for FOX-7 mixtures with GNPs capped with a) CTAB and b) Citrate, respectively.

for each test and plotted in Figure 15. The results confirmed that the optimum beam spot diameter was between 1.2 mm to 1.5 mm.

To determine the effect of powder density, the samples (6 mg) of sensitized FOX-7 with CTAB capped GNPs were filled in the sample holders (3 mm diameter) and gently pressed to various depths so that a set of pellets of various sample densities were prepared for ignition. A laser power of 46 W was used for each test. Following ignition, the ignition delay and full burn delay were measured, as seen in Figure 16. These results indicate that the ignition delay was not significantly affected by the sample density; however, the time to reach the ignition status of full burn was affected. When the sample density was high, e.g. $\geq 0.8\,g\,cm^{-3}$ which was about 42% of the theoretical maximum density (TMD) of FOX-7 ($1.885\,g\,cm^{-3}$), the full burn delay was getting stable and constantly short. Therefore, it is evident that relevantly higher compactness of the samples of the same mass will lead to faster laser initiation.

Through the laser ignition tests, the optical sensitizers were compared for their ignition effectiveness and efficiency in terms of threshold laser power to ignite and ignition delay. Although sensitized FOX-7 showed great enhancement in optical absorption for all these sensitizers, CTAB capped gold nanoparticles achieved much higher enhancement in laser ignitibility and was more suitable and effective for optical sensitizing in FOX-7. Higher concentration of CTAB capped GNPs than currently used is expected to further enhance laser

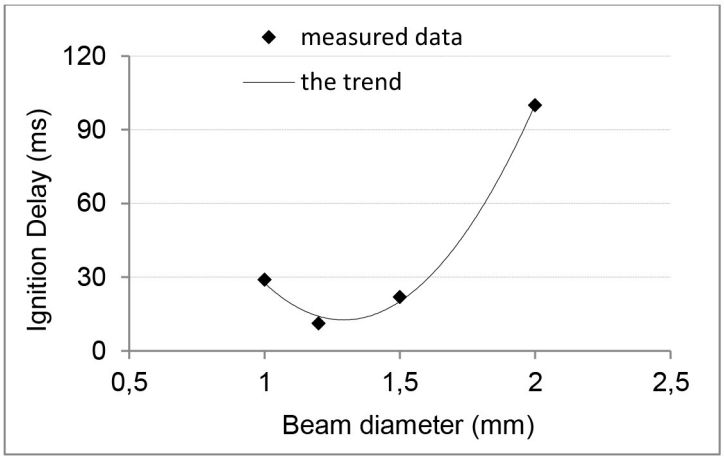

FIGURE 15 Ignition delay vs laser beam size.

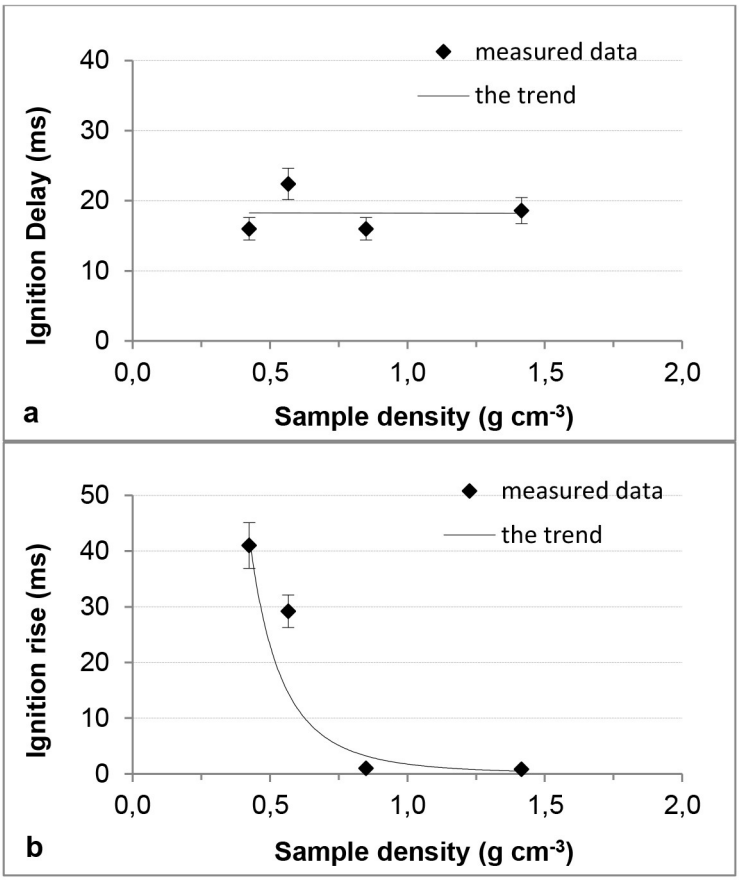

FIGURE 16 a) ignition delay and b) full burn delay vs sample density, respectively.

ignitibility of FOX-7. Therefore, above ignition results shows that the additive, GNPs with SPR at the wavelength of 808 nm significantly increase the ignition sensitivity of FOX-7 and its higher sample density shortens ignition rise time of the explosive.

3.4 | Laser initiator test

For the firing tests, the sensitized FOX-7 with 2 wt.% CTAB capped GNPs was used. A series of firings were made using the initiator test rig, in which the

nanoparticle-sensitised FOX-7 was placed against a booster pellet of a pure secondary explosive FOX-7 or RDX, respectively, and fired under strong confinement. A pre-formed bursting disk constituted the output stage of the device, with the intention that the bursting disk would be ejected at a speed sufficient to cause shock initiation in a third explosive pellet. It was decided that more data would be gathered if the velocity of the ejected bursting disk was measured, rather than by simply firing the device against a pellet of, for example, PETN. This simplified the experiments and allowed comparison between different design details to be quantified.

In each firing, the laser signals detected by the two photodiodes (see Figure 9 for firing arrangement) along with the signal triggered by the ejection of the bursting disk were recorded with a digitising oscilloscope, as shown in Figure 17, and the functioning time, i.e. the time duration from the onset of igniting laser to the ejection of the bursting disk, was measured. A laser power of 45 W was used for the test. A summary of the typical firings is given in Table 5, where RDX and FOX-7 were used as boosters respectively and bursting disc thickness was 200 μm as the confinement strength. The impact pressure produced by the bursting disc was transferred from the measured speed of the disc. Note that in all cases gold nanoparticle-sensitised FOX-7 was used as the initiating stage.

3.4.1 | Functioning time of the prototype

The functioning time of the prototype using FOX-7 as the booster (76 ms) was shorter than that using RDX (140 ms). The ignition delay times (11 ms) given in Figure 15 are much shorter than those observed in the prototype firings probably due to confinement. Furthermore, the burst disk velocity traces all show that the bursting of the initiator occurs very quickly (~100 μs) after the onset of motion of the disk. This suggests that the main delay in the functioning time of the prototype initiator is in the burning rate of the booster pellet, and the build-up of pressure required to burst the disc. The functioning of the prototype depends upon the rapid burning of the booster pellet, which leads to a build-up of pressure on the bursting disk, and ultimately breakage and ejection of the bursting disk at high speed. It is known that secondary explosives like FOX-7 burn relatively slowly at atmospheric pressure, and that the burn rate can be significantly increased if the pressure increases. It would be expected that the burning rate of FOX-7 would

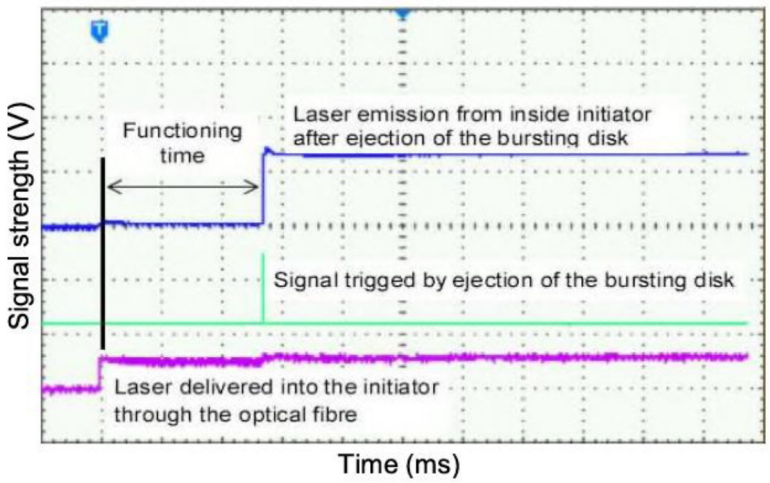

FIGURE 17 Ocilliscope traces for the measurement of functioning time.

TABLE 5 A summary of laser initiator firings.

Booster	Disc thickness (mm)	Functioning time (ms)	Bursting disk velocity (ms^{-1})	Impact pressure (GPa)
RDX	0.2	140	496	2.37
	0.4	88	353	1.58
FOX-7	0.2	76	481	2.28
	0.4	72	411	1.89

accelerate very quickly if burning was initiated within a perfectly sealed confinement. In this case at the onset of burning, gas is released which pressurises the confinement, leading to faster burning in a positive feedback mechanism that ends when the confinement is violently overcome. Thus, a better sealed confinement could be responsible for the improvement in the overall functioning time.

3.4.2 | Potential to initiate explosives

Gibbs & Popolato [22] gives shock initiation data for PETN at different densities, obtained by high-accuracy plane-wave impact experiments, and those data are reproduced below in Figure 18. As shown in Table 5 above, the bursting disks from the prototype initiator were ejected at the speed producing the impact pressures of 2.28 GPa and 2.37 GPa respectively, sufficient to detonate PETN specimen of 1.75 $g\,cm^{-3}$ pressed density. The Run-to-detonation distance is around 3 mm. These shock pressures are indicated on the Pop-plot below. It also shows that the impact pressure would also detonate HMX specimen of 1.89 $g\,cm^{-3}$ pressed density with a run-to-detonation distance of around 20 mm.

The ejection velocity of the bursting disk appears to be highest with disk thicknesses of 200 μm, and all experiments with thicker disks showed lower velocities, as shown previously in Table 5. This is contrary to expectation, because a thicker bursting disk would tend to yield a higher bursting pressure, and a more complete consumption of the booster pellet. The still photograph taken from high-speed video recordings of the experiments, shown in Figure 19, shows a cloud of burning material ejected from the experiment, which supports the view that not all of the booster material contributed to acceleration of the bursting disk. The lower ejection velocity with thicker bursting disks suggests that confinement failure occurred first at the interface between the glass window and the window retainer, rather than at the bursting disk. This seems plausible because the mechanical retention of the window in the thick-disk experiments only consisted of the relatively weak plastic insert. It is likely that an improved design in this area of the device would lead to higher disk ejection velocity.

These observations suggest that the prototype device could feasibly be used as the first stage in a slapper-type initiation device driven by a laser pulse, at least from the standpoint of the likely output stimulus that might be produced by this configuration. It would be advantageous for a final detonator-type device to include a true secondary explosive, rather than PETN, as the output stage, initiated by the laser-deflagration-driven initiator, and these firings show that improvements in the device design would be required to realise this goal.

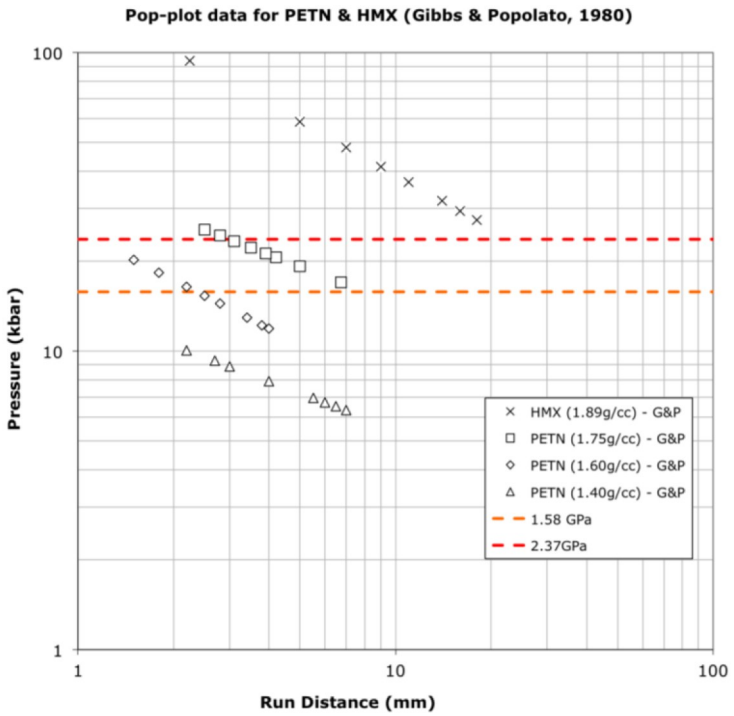

FIGURE 18 Run-to-detonation distance data for PETN and HMX, taken from Gibbs & Popolato. For reference, shock pressure of 2.37 GPa is shown with 1.58 GPa as a minimum required to detonate PETN specimen of 1.75 $g\,cm^{-3}$ pressed density.

FIGURE 19 Still frames taken at 1 ms intervals immediately prior to (the upper image) and following initiation (the lower image). The flash seen in the lower image indicates that the booster pellet was not completely consumed before confinement failed.

The prototype firings show that a two-stage laser-deflagration mechanism could feasibly be built as a detonator type device. In a multi-stage device of this type, the laser pulse would be used to initiate a small pellet of nanoparticle-sensitised material, which would initiate deflagration in a larger booster pellet under strong confinement. The burning of the booster would eject a high-speed pre-formed fragment, which would then impact, and shock initiate an output pellet. Although feasible, these experiments show that the prototype design here currently offers a functioning time of the order 70 ms, which is too long to be useful as a detonator. This long functioning time is attributed to the relatively weak confinement in the prototype, which limits the extent to which the burning rate can grow. It is expected that the overall functioning time could be reduced by improvements in the confinement strength in the area around the glass window, and by using a thicker bursting disk to promote burning of the booster to higher pressure.

4 | CONCLUSIONS

The present study in this paper has experimentally investigated the feasibility to optically sensitise an insensitive explosive FOX-7 by the doping of gold nanoparticles (GNPs) that strongly absorb at the wavelength of the incident laser (808 nm) and evaluated the enhanced laser ignitibility and detonation capability of the laser initiator devices. The conclusions from the study have also included the follows: gold nanoparticles capped with CTAB (Cetyltrimethyl ammonium bromide) were effective and efficient optical sensitizers for FOX-7; laser absorption and laser ignitibility increased with the doping content of GNPs; laser threshold power was reduced to ~8 W for a 2 wt.% GNPs content while a pure FOX-7 was not ignitable with a laser power of up to 46 W; the speed of the bursting disk ejected in the firing of the laser initiator was sufficient to cause shock initiation in a third explosive pellet, e.g. PETN, HMX. Therefore, it is evident that gold nanoparticles have been effective optical sensitizers. The significantly enhanced laser ignitibility of sensitized insensitive explosive with nanoparticles has made it feasible for such designed laser initiator to detonate a third secondary explosive in various applications.

ACKNOWLEDGEMENT

This study was funded by Dstl UK.

DATA AVAILABILITY STATEMENT

Data may be requested via the authors.

ORCID

Christopher Stennett http://orcid.org/0000-0002-6424-2549

REFERENCES

1. R. J. Spear, L. D. Redman, J. R. Bentley, Sensitization of High Density Silver Azide to Stab Initiation, MRL-R-881, Melbourne, Victoria: Defence Science and Technology Organisation, **1983**.
2. J. Akhavan, The Chemistry of Explosives, Royal Society of Chemistry, **2004**.
3. M. G. Wolfson, A Guide to Explosives Firing, DSTO-GD-0118, Melbourne, Victoria: DSTO, **1996**.
4. M. J. Caron, Reports of Premature Initiation of Electric Detonators by Radio Frequency Energy, Ontario: Explosives Risk Managers LLC, 202–288–2029, **2015**.
5. Q. Zeng, B. Li, M. Li, X. Wu, *Propellants Explos. Pyrotech.* **2016**, *41*, 864.
6. J. K. Cooper, C. D. Grant, J. Z. Zhang, *J. Phys. Chem. A* **2013**, *117*, 6043.
7. X. Fang, S. R. Ahmad, *Adv. Mater. Sci. Technol.* **2018**, *3*, 1–4.
8. L. Šimková, M. Šoral, K. Luspai, J. Ludvík, *J. Mol. Struct.* **2015**, *1083*, 10–16.
9. A. M. Turner, Y. Luo, J. H. Marks, R. Sun, J. T. Lechner, T. M. Klapötke, R. I. Kaiser, *J. Phys. Chem. A* **2022**, *126*, 4747.
10. X. Fang, A. J. Walton, *Opt. Laser Technol.* **2023**, *158*, 108767.
11. X. Fang, S. R. Ahmad, *Cent. Eur. J. Energ. Mater.* **2016**, *13*, 103.
12. X. Fang, W. G. McLuckie, *J. Hazard. Mater.* **2015**, *285*, 375.
13. E. Burke, *Ignition of Hexanitrostibene Type IV (HNS IV) by Diode Laser*, PhD thesis, Cranfield University, **2010**.
14. M. M. Alvarez, J. T. Khoury, T. G. Schaaf, M. N. Shafigullin, I. Vesmar, R. L. Whetten, *J. Phys. Chem. B* **1997**, *101*, 3706.
15. L. S. Jung, C. T. Campbell, T. M. Chinowsky, M. N. Mar, S. S. Yee, *Langmuir* **1998**, *14*, 5636.

16. K. E. Uhlenhake, D. Olsen, M. Gomez, M. Örnek, M. Zhou, S. F. Son, *Combust. Flame* **2021**, *233*, 111570.
17. P. R. West, S. Ishii, G. V. Naik, N. K. Emani, V. M. Shalaev, A. Boltasseva, *Laser Photonics Rev.* **2010**, *4*, 795.
18. D. Gérard, S. K. Gray, *J. Phys. D* **2015**, *48*, 184001.
19. A. Ziashahabia, R. Poursalehi, *Procedia Materials Science* **2015**, *11*, 434.
20. K. Kurihara, K. Suzuki, *Anal. Chem.* **2002**, *74*, 696.
21. T. A. El-Brolossy, T. Abdallah, M. B. Mohamed, S. Abdallah, K. Easawi, S. Negm, H. Talaat, *Eur. Phys. J. Spec. Top.* **2008**, *153*, 361.
22. T. R. Gibbs, A. Popolato, *University of California Press* **1980**, *4*, 291.

How to cite this article: X. Fang, C. Stennett, S. Gaulter, *Propellants, Explos., Pyrotech.* **2023**, *48*, e202300079. https://doi.org/10.1002/prep.202300079

Graphical Abstract

The contents of this page will be used as part of the graphical abstract of html only.
It will not be published as part of main.